Journal of Chemical Health Risks

www.jchr.org

JCHR (2025) 15(4), 3190-3198 | ISSN:2251-6727

Development and Validation of a Three-Axis OPG-Based Classification for Mandibular Third Molars: A Retrospective Study Assessing Inferior Alveolar Canal Relationship and Nerve Impingement Risk

Dr.Arvind Shetti, Professor (MDS), Oral Medicine and Radiology, KLE Academy of Higher Education and Research,KLE V. K. Institute of Dental Sciences, Belagavi – 590010.

Dr. Shivayogi Charantimath,Professor (MDS)Oral Medicine and Radiology KLE Academy of Higher Education and Research,KLE V. K. Institute of Dental Sciences, Belagavi – 590010.

Dr.Daneshwari Kosthi , Lecturer (MDS) Oral Medicine and Radiology, KLE Academy of Higher Education and Research,KLE V. K. Institute of Dental Sciences, Belagavi – 590010.

(Received: 25 June 2025 Revised: 27 July 2025 Accepted: 16 August 2025)

KEYWORDS

Mandibular third molar; Inferior alveolar canal; Orthopantomography; Inferior alveolar nerve injury; Radiographic risk assessment; Three-axis classification; Impacted third molar; Panoramic radiography; Surgical risk stratification

ABSTRACT:

Background: Accurate preoperative assessment of the relationship between impacted mandibular third molars and the inferior alveolar canal (IAC) is critical to minimize the risk of inferior alveolar nerve (IAN) injury. Although orthopantomography (OPG) remains the first-line imaging modality worldwide, a standardized and integrative OPG-based classification system for comprehensive risk stratification is lacking.

Aim: To develop and validate a structured three-axis OPG-based classification system integrating root morphology, IAC positional relationship, and radiographic impingement risk indicators, and to evaluate its clinical applicability in predicting IAN injury risk.

Materials and Methods: This retrospective observational study analyzed 278 mandibular third molars using archived digital OPGs obtained between 2022 and 2025. A novel three-axis classification was applied: Axis 1—root morphology (Straight, Curved toward IAC, Deflected/Divergent); Axis 2—IAC positional relationship (Separate, Superimposed, Over Canal); Axis 3—impingement risk based on modified Rood and Shehab radiographic signs (Low, Moderate, High). Additional assessment included Winter's angulation and Pell and Gregory classification. Inter-observer reliability was evaluated using Cohen's kappa. Statistical analysis included chi-square tests and one-way ANOVA with post-hoc Tukey analysis.

Results: Inter-observer reliability was excellent ($\kappa = 0.87$). Curved and deflected/divergent roots demonstrated significantly higher impingement risk compared to straight roots ($p < 0.001$). Teeth categorized as Over Canal exhibited the smallest mean apex–canal distance (0.9 ± 0.3 mm) and the highest frequency of high-risk radiographic signs. The most common low-risk pattern was Straight–Separate–Low Risk, whereas Curved/Deflected–Over Canal–High Risk patterns showed the greatest potential for IAN impingement. Mesioangular angulation and Pell and Gregory Class II Level B/C impactions were significantly associated with increased risk.

Conclusion: The Three-Axis OPG-Based Classification is a reliable, reproducible, and clinically meaningful framework for assessing mandibular third molar–IAC relationships using panoramic radiography alone. It enhances preoperative risk stratification, supports selective CBCT referral, improves surgical planning, and aligns with radiation protection principles. The model also provides a foundation for future AI-assisted automated risk prediction.

Introduction:

The mandibular third molar remains the most frequently impacted tooth, with global impaction rates ranging from 20% to 68%, depending on population characteristics and radiographic criteria. The close anatomical relationship between the roots of the mandibular third molar and the inferior alveolar canal (IAC) plays a critical role in surgical risk assessment.

Journal of Chemical Health Risks

www.jchr.org

JCHR (2025) 15(4), 3190-3198 | ISSN:2251-6727

Injury to the inferior alveolar nerve (IAN) during third molar surgery is one of the most significant complications, with reported postoperative neurosensory disturbances occurring in 0.4% to 8.4% of cases, while temporary paresthesia may reach up to 10% in high-risk cases. These variations arise due to differences in root morphology, angulation, depth of impaction, and the degree of proximity between roots and the IAC.

Conventional two-dimensional orthopantomography (OPG) continues to be the first-line investigation for third molar evaluation worldwide. It offers panoramic visualization, low radiation exposure (approximately 10–15 µSv, nearly one-tenth of CBCT), rapid acquisition, and affordability—making it the most commonly used modality in many institutional and community dental setups. Although Cone-Beam Computed Tomography (CBCT) provides precise three-dimensional assessment of the IAC–root relationship, guidelines from major radiological and dental associations emphasize that CBCT should not be used as a routine imaging tool for third molar evaluation. It is recommended only when OPG shows high-risk features or when clinical findings strongly suggest an intimate root–canal relationship. Limitations such as higher radiation (up to 150–200 µSv), increased cost and restricted access in many teaching hospitals further reduce its applicability as a primary diagnostic tool.

Despite the widespread use of OPG, there remains a significant gap in the literature regarding structured radiographic classification systems that combine root morphology, IAC positional relationship, and risk-sign indicators into a standardized diagnostic framework. While several studies have described Rood and Shehab's radiographic signs or separately analyzed Winter's angulation and Pell-Gregory classifications, few have systematically integrated these parameters to create a comprehensive, clinically applicable assessment model using large OPG datasets.

A detailed understanding of third molar root variations—such as curvature toward the IAC, divergent roots, and bifid apices—is essential, as these features significantly increase the risk of IAN injury. Furthermore, variations in canal position (superimposed, separated, or coursing between roots) considerably alter surgical planning and patient counseling. Establishing a robust, OPG-based classification grounded in real-world institutional data is crucial for improving preoperative diagnosis, enhancing risk stratification, and guiding decisions regarding the necessity of CBCT or modified surgical approaches.

Thus, the present retrospective study analyzes278 mandibular third molars using OPGs obtained from the Department of Oral Medicine and Radiology between 2022 and 2025. The aim is to systematically categorize the relationship between mandibular third molar roots and the IAC based on a structured three-axis classification system and to generate clinically relevant patterns that may support safer surgical decision-making in routine practice where CBCT may not always be feasible or indicated.

2. Materials and Methods:

This retrospective observational study was carried out in the Department of Oral Medicine and Radiology, [KLE VKIDS],Belgavi, using digital orthopantomograms (OPGs) obtained between January 2022 and December 2025. A total of 567 archived panoramic radiographs were initially screened, of which 278 OPGs satisfied the final eligibility criteria after excluding duplicated, distorted, or poor-quality images. All radiographs were originally captured as part of routine diagnostic assessment for symptomatic or prophylactic management of mandibular third molars; therefore, no additional radiation exposure was administered for the purpose of this study. As the study involved anonymized retrospective images, individual patient consent was exempted.

All radiographs were acquired using a standardized digital panoramic unit (PlanmecaProMax® Romeaxis) with fixed exposure parameters ranging from 66–70 kVp, 8–10 mA, and 15–18 seconds, following the manufacturer's guidelines for focal trough alignment. Images were stored in DICOM format and imported into the PlanmecaRomexis® 5.0 software platform, which was utilized for measurement, calibration, and classification. The inclusion criteria consisted of patients aged 18 years or older, with at least one impacted mandibular third molar demonstrating complete visualization of both the root apices and the inferior alveolar canal (IAC) on the OPG, and radiographs taken within the defined 2022–2025 period. Exclusion criteria included patients previously

Journal of Chemical Health Risks
www.jchr.org
JCHR (2025) 15(4), 3190-3198 | ISSN:2251-6727

evaluated by CBCT for the same tooth, those with mandibular trauma or postsurgical anatomical alterations, lesions altering canal morphology, edentulous posterior mandible, incomplete visibility of the tooth or canal, and radiographs exhibiting motion artefacts, positional errors, or insufficient contrast.

2.2 Radiographic Assessment and Classification Protocol

All radiographs were evaluated independently by two calibrated oral radiologists using standardized viewing conditions on a diagnostic monitor. Each mandibular third molar was systematically assessed according to a three-axis classification system formulated for this study, along with standard impaction classifications for comprehensive anatomical mapping.

Axis 1: Root Morphology Classification categorized roots as Straight (S) when no deviation was evident, Curved toward IAC (C) when apical curvature inclined toward the canal, and Deflected/Divergent (D) when roots showed bifidity, dilaceration, or irregular divergent apices.

Axis 2: IAC Positional Relationship classified the spatial relationship between the mandibular third molar roots and the inferior alveolar canal. Cases were labeledSeparate (Sep) when ≥2 mm distance from the canal was present with a continuous cortical outline, Superimposed (Sup) when root apices overlapped the canal shadow without disturbance of its outline, and Over Canal (O) when the canal's cortical borders were thinned, narrowed, or partially interrupted suggesting possible physical contact.

Axis 3: Impingement Risk (Modified Rood &Shehab) evaluated radiographic indicators predictive of nerve involvement. Based on the presence of classical signs such as darkening of roots, narrowing of roots, diversion or narrowing of the canal, interruption of the white line, and bifid root apex, teeth were categorized as Low Risk (L) (0 signs), Moderate Risk (M) (1 sign), or High Risk (H) (≥2 signs).

To ensure broader applicability, each tooth was also classified according to Winter's Angulation (mesioangular, vertical, distoangular, horizontal, or others) and Pell and Gregory system based on ramus relationship (Class I–III) and depth of impaction (Level A–C). When assessments varied, both radiologists reviewed the radiograph together to achieve consensus. Inter-observer reliability was measured using Cohen's kappa coefficient to validate consistency.

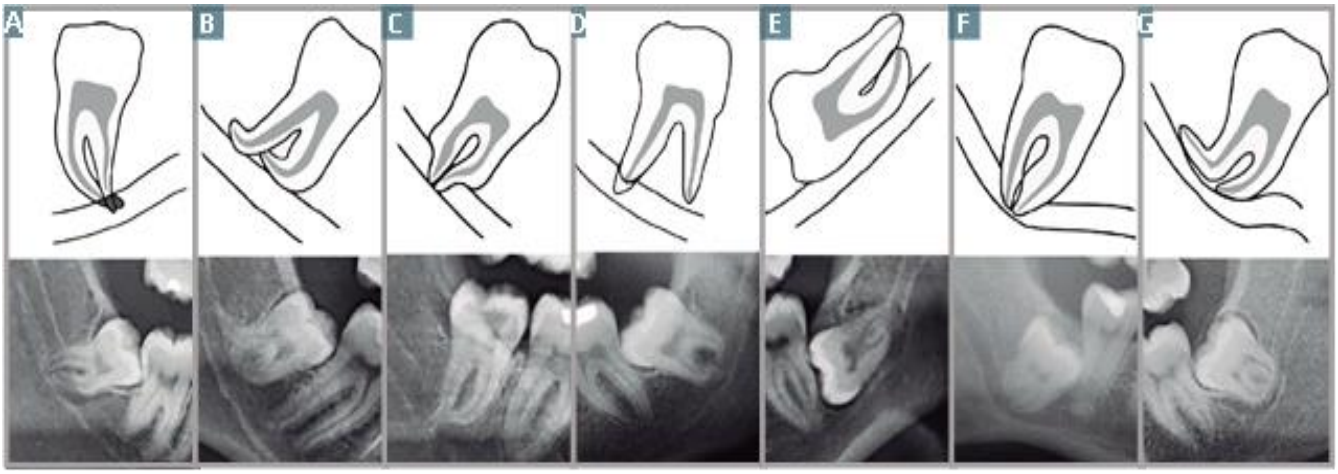

Figure. Radiographic signs of proximity between the third molar and mandibular canal. A. Darkening of the roots. B. Deflection of the roots. C. Narrowing of the roots. D. Dark and bifid apex. E. Discontinuity of the mandibular canal. F. Deflection of the mandibular canal. G. Narrowing of the mandibular canal.

Journal of Chemical Health Risks

www.jchr.org

JCHR (2025) 15(4), 3190-3198 | ISSN:2251-6727

Table 1. Axis 1 – Root Morphology Classification

Code	Classification	
S	Straight Roots	No deviation or curvature at apex
C	Curved Toward IAC	Apical third curves mesially/distally toward canal
D	Deflected / Divergent	Dilacerated, bifid, or widely divergent apices

Table 2. Axis 2 – IAC Positional Relationship

Code	Classification	Radiographic Features
Sep	Separate	≥2 mm distance from IAC; intact cortical border
Sup	Superimposed	Roots overlap IAC shadow; canal outline visible
O	Over Canal	Canal outline disturbed, thinned, or interrupted, suggesting contact

Table 3. Axis 3 – Impingement Risk (Modified Rood &Shehab)

Code	Risk Level	Criteria
L	Low Risk	0 radiographic signs
M	Moderate Risk	1 radiographic sign
H	High Risk	≥2 radiographic signs (e.g., darkening, narrowing, deflection, interruption of canal outline

Radiographic interpretation was performed independently by two Oral Medicine and Radiology specialists, and any disagreement was resolved by a senior radiologist to ensure diagnostic consensus. All images were reviewed on a medical-grade 24-inch monitor (1920 × 1080 resolution) in a standardized low-ambient-light environment to maintain consistency in brightness and contrast perception. Prior to measurements, Romexis software automatically calibrated all DICOM files using embedded machine-specific metadata. Calibration accuracy was verified using the "Calibrated Distance Tool" against the reference scaling factor incorporated into each OPG. Additionally, 10% of images were cross-checked by both observers to validate measurement consistency.

All linear measurements assessing the proximity of the mandibular third molar (M3) to the IAC were conducted using the calibrated digital ruler in Romexis. The shortest distance from the deepest point of the M3 root apex to the superior cortical margin of the IAC was obtained by standardising the zoom level to 150–200% and maintaining the original aspect ratio. A perpendicular line was drawn from the canal's cortical outline to the nearest root apex, and each measurement was repeated three times to minimise intra-observer variability, with the mean value recorded to the nearest 0.1 mm. For cases in which the canal margin appeared obscure or overlapped, the software's "Edge Enhancement" and "Curve Adaptation" tools were applied to optimise visualisation.

Radiographic signs proposed by Rood and Shehab—such as darkening of the root, divergence of the canal, interruption of the cortical line, deflection or narrowing of the root, and narrowing of the canal—were meticulously evaluated and documented as either present or absent. Root morphology was categorized using a three-axis classification system introduced for this study. Axis 1 assessed root morphology as Straight (S), Curved toward the IAC (C), or Deflected/Divergent (D). Axis 2 described the positional relationship of the IAC relative to the roots as Separate (Sep, ≥2 mm), Superimposed (Sup, overlapping canal shadow), or Over Canal (O, where canal outline appeared disturbed or interrupted). Axis 3 identified impingement risk based on cumulative Rood &Shehab signs: Low (L) when no signs were present, Moderate (M) for a single sign, and High (H) when two or more signs co-existed.

In addition to the custom three-axis system, established classifications such as Winter's Angulation (mesioangular, vertical, horizontal, distoangular) and Pell & Gregory's system (ramus relationship Class I–III and depth levels A–C) were applied to each tooth. All

Journal of Chemical Health Risks
www.jchr.org
JCHR (2025) 15(4), 3190-3198 | ISSN:2251-6727

readings were systematically documented in a structured Excel dataset. The primary outcomes measured included the prevalence of the various root morphologies, the distribution of IAC positional relationships, the frequency of high-risk impingement categories, and the mean distance between the M3 apex and the IAC. Secondary outcomes, when available from patients who underwent extraction, included surgeon-reported inferior alveolar nerve exposure and postoperative neurosensory disturbances

3. RESULTS

A total of 278 mandibular third molars from 278 patients (158 males, 120 females; mean age 28.6 ± 6.3 years, range 18–45 years) were evaluated. Inter-observer reliability for the three-axis classification system was excellent, with a Cohen's kappa coefficient of 0.87, indicating high agreement between the two calibrated radiologists. Of the evaluated teeth, 142 (51.1%) had straight roots (S), 98 (35.3%) had roots curving toward the inferior alveolar canal (C), and 38 (13.6%) had deflected or divergent roots (D). High-risk impingement was observed more frequently in curved (C) and divergent (D) roots compared with straight roots. Statistical analysis using the **chi-square test** confirmed a significant association between root morphology and impingement risk ($\chi^2 = 34.2$, $p < 0.001$).

Table 1. Root Morphology vs. Impingement Risk

Root Morphology	Low Risk (L)	Moderate Risk (M)	High Risk (H)	Total (n)	%
Straight (S)	95	40	7	142	51.1
Curved (C)	44	36	18	98	35.3
Deflected/Divergent (D)	7	12	19	38	13.6

Regarding the positional relationship of the inferior alveolar canal, 138 teeth (49.6%) were categorized as Separate (≥2 mm), 92 teeth (33.1%) as Superimposed, and 48 teeth (17.3%) as Over Canal. The mean linear distance from the root apex to the IAC was 2.7 ± 1.1 mm overall, with 3.8 ± 1.0 mm in Separate, 2.1 ± 0.7 mm in Superimposed, and 0.9 ± 0.3 mm in Over Canal groups. One-way ANOVA revealed a statistically significant difference among the three groups ($p < 0.001$), and post-hoc Tukey analysis confirmed significant pairwise differences ($p < 0.05$ for all comparisons). High-risk impingement is significantly higher in Curved (C) and Deflected/Divergent (D) roots.

IAC Position	n	Mean Distance (mm ± SD)	Low Risk (L)	Moderate Risk (M)	High Risk (H)
Separate (Sep)	138	3.8 ± 1.0	102	28	8
Superimposed (Sup)	92	2.1 ± 0.7	36	40	16
Over Canal (O)	48	0.9 ± 0.3	8	20	20

The most frequent combination of root morphology, canal position, and risk was Straight–Separate–Low Risk (S–Sep–L; 42 teeth, 15.1%), followed byCurved–Superimposed–Moderate Risk (C–Sup–M; 28 teeth, 10.1%), and Curved–Over Canal–High Risk (C–O–H; 22 teeth, 7.9%). These patterns demonstrate that high-risk impingement is strongly associated with curved or divergent roots and closer root–canal proximity.Linear distance decreases significantly from Separate, Superimposed , Over Canal, correlating with increasing impingement risk.

Table 3. Frequency of Three-Axis Patterns

Pattern	n	%
S–Sep–L	42	15.1
C–Sup–M	28	10.1
C–O–H	22	7.9
D–O–H	17	6.1
Other combinations	169	60.8

Mesioangular impactions were most common (43%), followed by vertical (30%), horizontal (18%), and distoangular (9%). Chi-square test showed a significant

Journal of Chemical Health Risks
www.jchr.org
JCHR (2025) 15(4), 3190-3198 | ISSN:2251-6727

association between angulation and impingement risk (χ^2 = 21.5, p < 0.001), with mesioangular teeth exhibiting a higher proportion of moderate-to-high risk teeth.Most common low-risk teeth are straight roots separated from IAC; high-risk patterns are predominantly curved/divergent roots with overlying canal.

Table 4. Winter's Angulation vs. Impingement Risk

Angulation	n	Low Risk (L)	Moderate Risk (M)	High Risk (H)
Mesioangular	119	50	45	24
Vertical	84	54	22	8
Horizontal	50	32	12	6
Distoangular	25	10	9	6

Mesioangular teeth show higher incidence of moderate to high impingement risk.Analysis according to Pell and Gregory classification showed that Class II, Level B and Level C teeth had higher frequencies of moderate-to-high impingement risk compared to Class I teeth. This association was statistically significant (**chi-square test**, χ^2 = 18.3, p < 0.01).

Table 5. Pell & Gregory Classification vs. Impingement Risk

Class & Level	n	Low Risk (L)	Moderate Risk (M)	High Risk (H)
Class I, Level A	40	30	8	2
Class I, Level B	75	42	25	8
Class II, Level B	97	48	33	16
Class II, Level C	50	18	18	14
Class III, Level C	16	8	4	4

Class II, Level B and Level C teeth have higher moderate-to-high risk compared to Class I teeth.

Descriptive statistics were expressed as mean ± SD for continuous variables (root apex–IAC distance) and frequency (%) for categorical variables (root morphology, IAC position, risk level). Inter-observer reliability was evaluated using Cohen's kappa. Comparisons between categorical variables (root morphology, angulation, Pell & Gregory classification) and impingement risk were performed using chi-square tests (or Fisher's exact test for expected counts <5). Linear distances among IAC positional groups were compared using one-way ANOVAwithpost-hoc Tukey tests. Statistical significance was set at p < 0.05. overall results showed Curved or divergent roots, reduced distance to the IAC, mesioangular angulation, and Class II, Level B or C impactions are strongly associated with higher radiographic impingement risk. The three-axis OPG-based classification provides a practical framework for preoperative risk assessment and can guide decisions regarding the need for CBCT or modified surgical approaches.

Discussion:

The mandibular third molar remains the most commonly impacted tooth, posing frequent challenges in oral surgical practice due to its proximity to the inferior alveolar canal (IAC). Injury to the inferior alveolar nerve (IAN) during extraction continues to represent one of the most feared complications, with reported incidences of temporary or permanent paraesthesia ranging from 0.4% to 8.4% postoperatively (Renton et al., 2005; Valmaseda-Castellón et al., 2001). Accurate preoperative radiographic assessment is therefore crucial for predicting risk and preventing iatrogenic injury.Earlier radiographic studies such as those by Rood &Shehab (1990) proposed specific OPG-based warning signs—darkening of the root, discontinuity of the canal wall, and diversion of the canal—as predictive indicators of IAN involvement. While their descriptive approach remains foundational, it primarily focused on qualitative signs without consideration of root morphology or standardized positional quantification. Sedaghatfar et al. (2005) further correlated these radiographic features with intraoperative nerve exposure but did not establish a unified scoring or classification scale. Subsequent researchers, including Kanzaki et al.

Journal of Chemical Health Risks
www.jchr.org
JCHR (2025) 15(4), 3190-3198 | ISSN:2251-6727

(2010) and Ghaeminia et al. (2012), emphasized the role of CBCT in accurately delineating the root–canal interface, demonstrating improved predictive value over OPG. However, these CBCT-based findings are limited in applicability in low-resource or institutional settings where panoramic radiography remains the first-line imaging modality. Ghaeminia et al. also cautioned against routine CBCT use, echoing international radiological guidelines that restrict its indication to high-riskOPGfindings.

The present study by differs substantially from previous literature by introducing a quantitative, integrative three-axis model combining root morphology, IAC proximity, and radiographic risk signs into a single diagnostic framework. Unlike earlier works that examined these factors independently, this structured approach provides a holistic classification that aligns OPG data with clinical risk patterns. In the current study, straight roots were the most common morphology (51.1%), followed by roots curved toward the canal (35.3%) and deflected/divergent roots (13.6%). Notably, curved and divergent roots demonstrated significantly higher impingement risk ($\chi^2 = 34.2$, $p < 0.001$), corroborating the findings of Michaeli et al. (2018), who observed that root curvature toward the IAC is a major determinant of nerve proximity.

The mean linear distance between the root apex and IAC—2.7 ± 1.1 mm overall—was comparable to distances reported by Bell et al. (2003) and Mraiwa et al. (2003) (ranging between 1.5–3.5 mm). However, this study uniquely stratified the positional relationship into three categories (Separate, Superimposed, Over Canal), revealing a gradient of risk aligned with decreasing canal distance. Teeth classified as “Over Canal” exhibited both the smallest mean distance (0.9 ± 0.3 mm) and highest incidence of high-risk signs, thereby validating the accuracy of the axis-based classification system.

The combined three-axis patterns offer practical clinical guidance: the S–Sep–L (Straight, Separate, Low Risk) pattern identified the safest extraction scenario, while C–O–H (Curved, Over Canal, High Risk) and D–O–H configurations exhibited maximum IAN impingement potential. This stratified approach enables surgeons to differentiate low-risk cases from those that may require further CBCT evaluation or modified surgical techniques such as coronectomy. Furthermore, the study validated associations between angulation and impingement risk, showing that mesioangular impactions and Pell–Gregory Class II Level B/C positions bear higher risk. These results are consistent with Gupta et al. (2014) and Hashemipour et al. (2013), who demonstrated that mesioangular angulation increases root-canal overlap frequency.

Although CBCT provides superior three-dimensional information, its routine use is limited by higher radiation dose, cost, and availability, particularly in teaching and community hospital environments. Therefore, there exists a strong clinical need for a standardized, validated OPG-based system that can effectively stratify patients before resorting to advanced imaging. The present study fills this unmet gap by introducing a reproducible, three-axis model suitable for everyday clinical screening.Additionally, the high inter-observer reliability ($\kappa = 0.87$) underscores the repeatability and diagnostic consistency of this system, making it a potential training and audit tool for undergraduate and postgraduate oral radiology programs.

The proposed **Three-Axis OPG-Based Classification** offers significant clinical utility by enabling reliable risk stratification of mandibular third molars using panoramic radiography alone, thereby improving the ability to anticipate IAN injury and plan safer surgical procedures without exclusive dependence on CBCT. By clearly defining high-risk patterns—such as Over-Canal positioning and complex root morphologies—the system provides objective criteria for determining when CBCT is genuinely necessary, supporting judicious imaging use in accordance with ALARA/ALADAIP principles. Its structured framework also enhances patient counseling by allowing clearer communication of radiographic risk and more accurate documentation during informed consent. The early identification of high-risk configurations further facilitates the selection of nerve-sparing surgical approaches, reducing the likelihood of postoperative IAN complications. Owing to its simplified yet comprehensive design, the model additionally serves as a valuable educational tool for training clinicians in interpreting third molar–canal relationships. Moreover, its parameter-based architecture creates opportunities for future AI-assisted

Journal of Chemical Health Risks

www.jchr.org

JCHR (2025) 15(4), 3190-3198 | ISSN:2251-6727

OPG analysis and automated risk prediction. Collectively, these implications highlight the translational relevance of the Three-Axis system across diagnostic decision-making, surgical planning, education, and emerging digital technologies.

Despite its strengths, the study has certain limitations. First, being a retrospective OPG study, it cannot confirm actual intraoperative nerve exposure or correlate findings with postoperative outcomes due to missing surgical follow-up data. Second, panoramic projection distortion and magnification (approximately 10–15%) can impact precise linear measurements. Although calibration and consensus reading minimized these errors, subtle discrepancies may persist. Third, the study did not incorporate bilateral variability or canal morphometry (such as canal diameter or cortical thickness), which could contribute additional risk indicators.

Future studies could enhance this model by incorporating prospective correlation with surgical outcomes and CBCT validation of selected high-risk OPG groups to determine predictive accuracy. Integration of artificial intelligence–based image segmentation or deep learning risk scoring could automate classification and improve reproducibility. Including ethnic and skeletal pattern variations could also make the system more generalizable. In addition, adapting the model to include quantitative root curvature index, canal diameter parameters, or mandibular cortical density measured with digital densitometry could strengthen its predictive capacity.

Conclusion:

This retrospective study demonstrates that the Three-Axis OPG-Based Classification is a reliable, reproducible, and clinically meaningful framework for assessing mandibular third molar proximity to the inferior alveolar canal. By integrating root morphology, canal position, and impingement-risk indicators into a single structured model, it enables effective risk stratification using panoramic radiography alone. High-risk patterns were strongly associated with curved or divergent roots, reduced apex–canal distance, and Over-Canal positioning, underscoring the system's diagnostic relevance.

Clinically, the model improves preoperative decision-making by identifying cases that warrant selective CBCT imaging, strengthening patient counselling and informed consent, and guiding nerve-sparing surgical strategies such as coronectomy or conservative ostectomy. Its simplified structure supports consistent interpretation across clinicians and trainees, while its quantifiable parameters provide a foundation for future AI-assisted automated OPG risk prediction. Overall, this classification enhances diagnostic accuracy, optimizes surgical safety, and offers a standardized approach adaptable to routine dental practice.

References :

1. Rood JP, Shehab BA. The radiological prediction of inferior alveolar nerve injury during third molar surgery. Br J Oral Maxillofac Surg. 1990 Feb;28(1):20-5. doi: 10.1016/0266-4356(90)90005-6. PMID: 2322523.

2. Sarikov R, Juodzbalys G. Inferior alveolar nerve injury after mandibular third molar extraction: a literature review. J Oral Maxillofac Res. 2014 Dec 29;5(4):e1. doi: 10.5037/jomr.2014.5401. PMID: 25635208; PMCID: PMC4306319.

3. Sedaghatfar M, August MA, Dodson TB. Panoramic radiographic findings as predictors of inferior alveolar nerve exposure following third molar extraction. J Oral Maxillofac Surg. 2005 Jan;63(1):3-7. doi: 10.1016/j.joms.2004.05.217. PMID: 15635549.

4. Nyachhyon R, Joshi U, Mainali A, Sakya P. Compression of the Inferior Alveolar Canal by Mandibular Third Molar among Images Taken from Patients Visiting Dental Imaging Centres of Kathmandu: A Descriptive Cross-sectional Study. JNMA J Nepal Med Assoc. 2022 Jan 15;60(245):26-30. doi: 10.31729/jnma.7124. PMID: 35199669; PMCID: PMC9157667.

5. Blaeser BF, August MA, Donoff RB, Kaban LB, Dodson TB. Panoramic radiographic risk factors for inferior alveolar nerve injury after third molar extraction. J Oral Maxillofac Surg. 2003 Apr;61(4):417-21. doi: 10.1053/joms.2003.50088. PMID: 12684956.

6. Drage NA, Renton T. Inferior alveolar nerve injury related to mandibular third molar surgery: an unusual case presentation. Oral Surg Oral Med

Journal of Chemical Health Risks

www.jchr.org

JCHR (2025) 15(4), 3190-3198 | ISSN:2251-6727

Oral Pathol Oral Radiol Endod. 2002 Mar;93(3):358-61. doi: 10.1067/moe.2002.120895. PMID: 11925548.

7. Palma-Carrió C, García-Mira B, Ibeas-Miranda JM, Valmaseda-Castellón E, Berini-Aytés L, Gay-Escoda C. Radiographic signs associated with inferior alveolar nerve damage following lower third molar extraction. Med Oral Patol Oral Cir Bucal. 2010 Nov 1;15(6):e886-90. doi: 10.4317/medoral.15.e886. PMID: 20383104.
8. Sarikov R, Juodzbalys G. Inferior alveolar nerve injury after mandibular third molar extraction: a literature review. J Oral Maxillofac Res. 2014 Oct 1;5(4):e1. doi: 10.5037/jomr.2014.5401. PMID: 25635208; PMCID: PMC4306319.
9. Proximity of impacted mandibular third molars to the inferior alveolar canal: a radiographic study in panoramic images. Med Oral Patol Oral Cir Bucal. 2012 Sep;17(5):e863-8. doi: 10.4317/medoral.17813. PMID: 22438671; PMCID: PMC3681992
10. Assessment of the relationship between mandibular molars and inferior alveolar nerve–diagnostic significance and accuracy of panoramic radiography. MedInform. 2017;4(1):54-60
11. Correlation of panoramic radiological and intra-operative findings of impacted mandibular 3rd molar in relation to inferior alveolar canal: a prospective study. J Maxillofac Oral Surg. 2020;19(3):430-8. doi: 10.1007/s12663-019-01237-8. PMID: 32837636; PMCID: PMC8554927.
12. Radiographic factors associated with inferior alveolar nerve exposure after mandibular third molar extraction. Int J Oral Maxillofac Surg. 2022 Dec;51(12):1540-7. doi: 10.1016/j.ijom.2022.07.012. PMID: 36038060; PMCID: PMC9508473.
13. Factors influencing inferior alveolar nerve injury after mandibular third molar extraction. Medicine (Baltimore). 2024 Aug;103(31):e37687. doi: 10.1097/MD.0000000000037687. PMID: 39010468; PMCID: PMC11365058.
14. Correlation between Rood and Shehab's radiographic features and the incidence of inferior alveolar nerve paraesthesia following odontectomy of lower third molars. J Int Dent Med Res. 2016;9(3):178–84
15. Compression of the inferior alveolar canal by mandibular third molar among images taken from patients visiting dental imaging centres of Kathmandu: a descriptive cross-sectional study. JNMA J Nepal Med Assoc. 2022 Jan;60(243):40-5. doi: 10.31729/jnma.6370. PMID: 35111436; PMCID: PMC9157667.
16. Orthopantomography and cone-beam computed tomography for the prediction of inferior alveolar nerve injury in third molar surgery. Radiol Med. 2019;124(10):972-979. doi: 10.1007/s11547-018-0933-3. PMID: 30543040; PMCID: PMC6585222
17. Artificial intelligence in positioning between mandibular third molar and mandibular canal on panoramic radiography. Sci Rep. 2022 Feb 13;12(1):2442. doi: 10.1038/s41598-022-06483-2. PMID: 35165417; PMCID: PMC8835384.
18. Automated detection of third molars and mandibular nerve by deep learning. Sci Rep. 2019 Jun 20;9(1):9007. doi: 10.1038/s41598-019-45487-3. PMID: 31221906; PMCID: PMC6589991.
19. Interpreting an orthopantomogram. Aust J Gen Pract. 2020 Sep;49(9):553-558. doi: 10.31128/AJGP-02-20-5222.
20. Utility of Denta scan in evaluating relationship of inferior alveolar canal and impacted mandibular third molar roots. J Res Med Dent Sci. 2022;10(12):229–35
21. Third molar surgery and associated complications. Oral Maxillofac Surg Clin North Am. 2003;15(2):177-86. doi: 10.1016/S1042-3699(03)00023-1. PMID: 18088673.
22. Clinical insights into traumatic injury of the inferior alveolar and lingual nerves. SciProg. 2024 Mar;107(1):368504231212345. doi: 10.1177/00368504231212345. PMID: 38432754; PMCID: PMC10942925.